

Supporting Information

Intrinsic doping limit and defect-assisted luminescence in Cs_4PbBr_6

Young-Kwang Jung,[†] Joaquín Calbo,[‡] Ji-Sang Park,[‡] Lucy D. Whalley,[‡]

Sunghyun Kim,[‡] and Aron Walsh^{*,†,‡}

[†]*Department of Materials Science and Engineering, Yonsei University, Seoul 03722, Korea*

[‡]*Department of Materials, Imperial College London, Exhibition Road, London SW7 2AZ,*

UK

E-mail: a.walsh@imperial.ac.uk

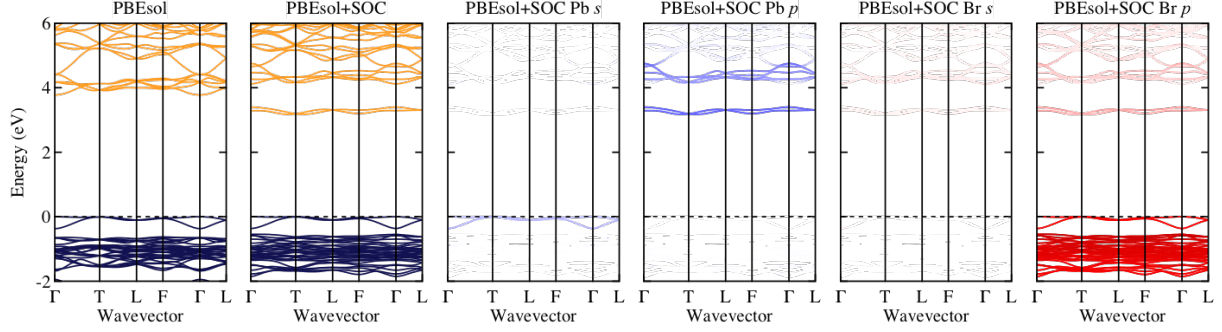


Figure S1: Orbital projected band structures calculated from PBEsol(+SOC). Band splitting is observed for lower conduction bands after spin-orbit coupling (SOC) was included in the calculation. Valence band maximum was set to 0 eV. Upper valence bands are composed of Pb 6s and Br 4p orbitals whereas lower conduction bands are composed of Pb 6p and Br 4p orbitals.

Surface calculations

For surface calculations of $\text{Cs}_4\text{PbBr}_6(110)$, symmetric slab model was considered with 25 atomic layers and vacuum region of 15 \AA . The plane-wave kinetic cutoff energy of 700 eV and Γ -centred k -point grid of $4 \times 3 \times 1$ was used. Full atomic relaxation of the slab was performed where the innermost five atomic layers were fixed at their bulk values.

The surface energy (E_{surf}) was calculated following

$$E_{\text{surf}} = \frac{1}{2A} \left[E_{\text{slab}}^{\text{rel}} - \frac{N_{\text{slab}}^{\text{atom}}}{N_{\text{bulk}}^{\text{atom}}} E_{\text{bulk}} \right] \quad (1)$$

where $E_{\text{slab}}^{\text{rel}}$ and E_{bulk} are the total energy of relaxed slab and bulk, $N_{\text{slab}}^{\text{atom}}$ and $N_{\text{bulk}}^{\text{atom}}$ are the number of atoms in the slab and bulk. The use of symmetric surface slab models necessitates a factor of 1/2.

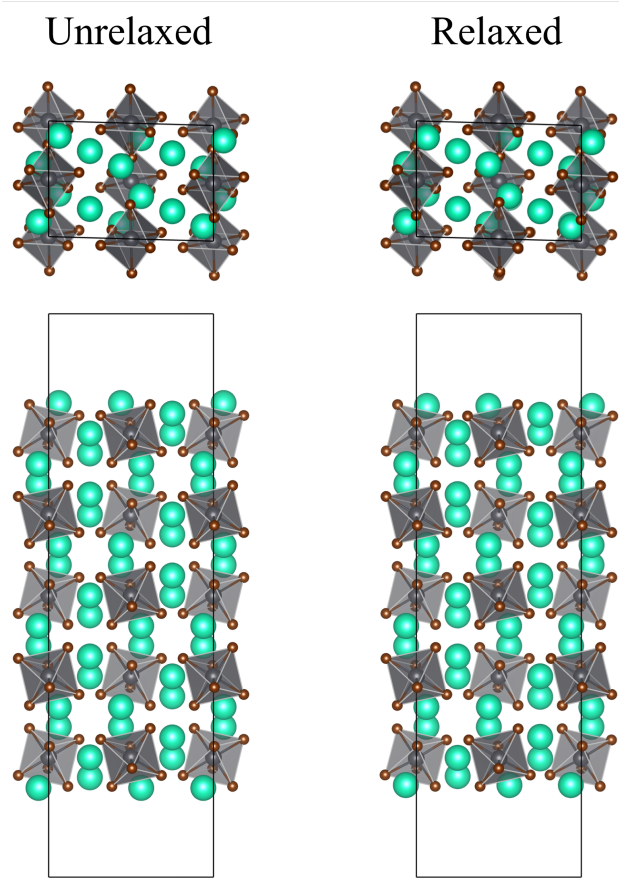


Figure S2: Atomic structure of unrelaxed and relaxed surface slab model of $\text{Cs}_4\text{PbBr}_6(110)$. Both top view (upper figures) and side view (lower figures) are shown.

Defect calculations

To maintain stable Cs_4PbBr_6 phase in thermodynamic equilibrium growth conditions, the chemical potential of Cs, Pb, and Br should satisfy

$$4\mu_{\text{Cs}} + \mu_{\text{Pb}} + 6\mu_{\text{Br}} = \Delta H_{\text{f}}(\text{Cs}_4\text{PbBr}_6) = -17.45 \text{ eV} \quad (2)$$

where μ_i is the atomic chemical potential of constitute element i and $\Delta H_{\text{f}}(j)$ is the formation energy of compound j . To avoid existence of secondary phases, inequalities below must also be satisfied

$$\mu_{\text{Cs}} + \mu_{\text{Pb}} + 3\mu_{\text{Br}} < \Delta H_{\text{f}}(\text{CsPbBr}_3) = -6.46 \text{ eV} \quad (3)$$

$$\mu_{\text{Cs}} + 2\mu_{\text{Pb}} + 5\mu_{\text{Br}} < \Delta H_{\text{f}}(\text{CsPb}_2\text{Br}_5) = -9.28 \text{ eV} \quad (4)$$

$$4\mu_{\text{Cs}} + 9\mu_{\text{Pb}} < \Delta H_{\text{f}}(\text{Cs}_4\text{Pb}_9) = -2.68 \text{ eV} \quad (5)$$

$$\mu_{\text{Cs}} + \mu_{\text{Br}} < \Delta H_{\text{f}}(\text{CsBr}) = -3.58 \text{ eV} \quad (6)$$

$$\mu_{\text{Pb}} + 2\mu_{\text{Br}} < \Delta H_{\text{f}}(\text{PbBr}_2) = -2.67 \text{ eV} \quad (7)$$

The chemical potential satisfying Eqns. (2-7) are shown as the shaded region in Figure 1e.

The formation energy of neutral defects, $\Delta H_d(\alpha, 0)$, was calculated following

$$\Delta H_d(\alpha, 0) = E(\alpha, 0) - E(\text{host}) + \sum_i n_i (E_i + \mu_i) \quad (8)$$

where $E(\alpha, 0)$ and $E(\text{host})$ are total energy of supercell with a point defect α and perfect supercell, E_i stands for the the total energy of pure elemental solid of element i which is reference for μ_i , and n_i is the number of i atom exchanged between the perfect supercell and the thermodynamic reservoir when defect α forms. Calculated neutral defect formation energies are tabulated in Table S1. It is worth mentioning that the equilibrium defect concentration can not be estimated by the neutral defect formation energy as the neutral defect

formation energy doesn't take account of the electronic chemical potential (Fermi level).

Table S1: Formation energy of point defects (in unit of eV) of Cs_4PbBr_6 at points A, B, and C in chemical potential space (Figure 1e).

V_{Cs}	V_{Pb}	V_{Br}	Pb_{Cs}	Br_{Cs}	Cs_{Pb}	Br_{Pb}	Cs_{Br}	Pb_{Br}	Cs_i	Pb_i	Br_i
A: $\mu_{\text{Cs}} = -3.62$, $\mu_{\text{Pb}} = -2.96$, $\mu_{\text{Br}} = 0.00$											
0.93	2.25	3.45	2.18	0.16	1.78	1.49	7.09	7.09	3.78	5.24	0.72
B: $\mu_{\text{Cs}} = -2.88$, $\mu_{\text{Pb}} = -1.48$, $\mu_{\text{Br}} = -0.74$											
1.67	3.74	2.71	1.44	1.65	2.52	3.72	5.61	4.85	3.04	3.75	1.47
C: $\mu_{\text{Cs}} = -2.13$, $\mu_{\text{Pb}} = 0.00$, $\mu_{\text{Br}} = -1.49$											
2.42	5.23	1.96	0.70	3.14	3.27	5.96	4.12	2.62	2.29	2.27	2.21

Table S2: Self-consistent Fermi level (in unit of eV) and concentration of charge carriers and point defects (in unit of cm^{-3}) of Cs_4PbBr_6 at points A, B, and C in chemical potential space (Figure 1e).

	A	B	C
E_{F}	0.897405	1.64186	2.38636
e^-	3.45×10^{-34}	1.11×10^{-21}	3.56×10^{-09}
h^+	7.08×10^5	2.21×10^{-07}	6.87×10^{-20}
V_{Cs}	1.14×10^{15}	1.13×10^{15}	1.13×10^{15}
V_{Pb}	1.11×10^{-5}	1.11×10^{-5}	1.11×10^{-5}
V_{Br}	4.82×10^{-5}	4.83×10^{-5}	4.83×10^{-5}
Pb_{Cs}	1.14×10^{15}	1.13×10^{15}	1.13×10^{15}
Br_{Cs}	4.84×10^{18}	3.92×10^{-02}	2.79×10^{-02}
Cs_{Pb}	3.14×10^3	3.15×10^3	3.15×10^3
Br_{Pb}	8.79×10^4	8.55×10^{-21}	5.09×10^{-28}
Cs_{Br}	1.05×10^{-36}	1.06×10^{-36}	3.74×10^{-36}
Pb_{Br}	3.23×10^{-50}	3.49×10^{-49}	1.22×10^{-22}
Cs_i	8.54×10^0	8.56×10^0	8.56×10^0
Pb_i	2.98×10^{-39}	1.12×10^{-38}	5.66×10^{-17}
Br_i	3.49×10^{11}	3.44×10^{11}	3.44×10^{11}

Table S3: Frequency (in cm^{-1}) of the vibrational modes in polybromide species. Infrared (left) / Raman (right) intensities are given within parenthesis.

	ν_1	ν_2	ν_3
Br_3^-	78 (0.3/0.0)	156 (430.3/0.0)	168 (0.0/155.5)
Br_3^{2-}	68 (276.7/0.5)	83 (0.2/490.0)	94 (0.5/324.2)

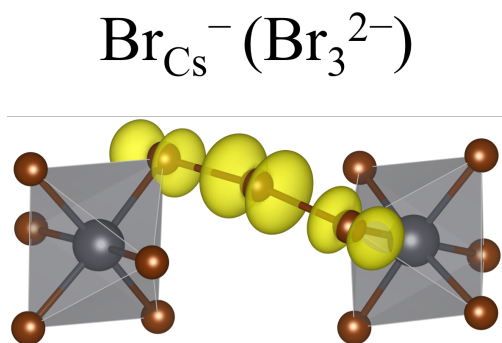


Figure S3: Calculated spin density plot of $\text{Br}_{\text{Cs}}^- (\text{Br}_3^{2-})$ where up spin electron fills anti-bonding orbital.

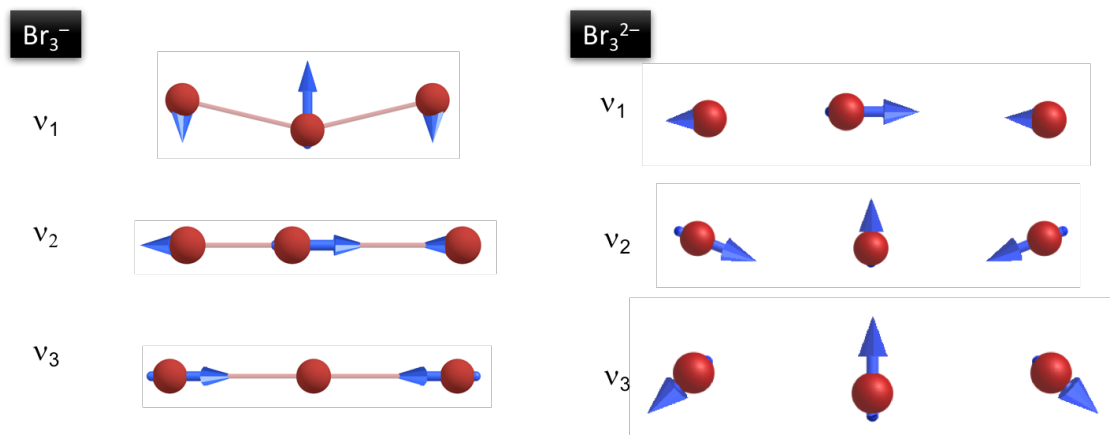


Figure S4: The vibrational modes in polybromide species. The direction of displacement vectors are indicated by blue arrows.

Table S4: Energy (E) and oscillator strength (f) for the lowest-lying same-spin electronic transition in different states of tribromide species.

	E (nm)	E (eV)	f
$\text{Br}_3^-(180^\circ)$	401	3.09	0.000
$\text{Br}_3^-(170^\circ)$	411	3.02	0.012
$\text{Br}_3^-(160^\circ)$	443	2.80	0.037
Br_3^{2-}	822	1.51	0.003
Br_3^{3-}	99	12.54	0.000

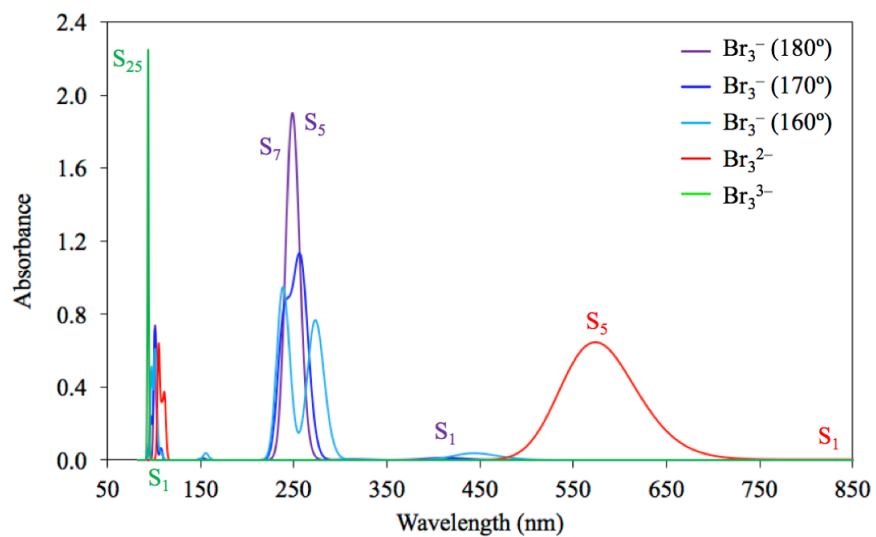


Figure S5: Simulated absorption spectra for the different polybromide anions. Characteristic electronic excitations (S_n) are indicated.

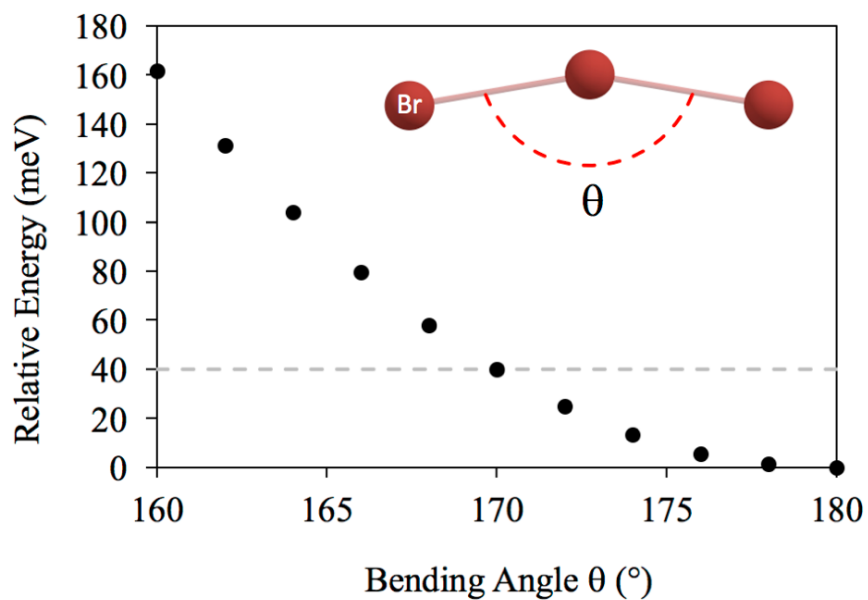


Figure S6: Energy penalty required to distort Br_3 from linearity as a function of the internal bending angle θ .

Table S5: Energy difference (in eV) between the first excited state (S_1) and the ground state (S_0) for the tribromide species as a function of the Br-Br distance (in Å). Br-Br distance of Br_3^- and Br_3^{2-} in their ground state is 2.56 Å and 3.21 Å, respectively.

Br-Br	Br_3^-	Br_3^{2-}	Br_3^{3-}
2.50	3.40	3.62	6.84
2.56	3.11	3.37	7.29
2.60	2.92	3.20	7.59
2.70	2.50	2.83	8.19
2.80	2.13	2.49	8.68
2.90	1.81	2.20	9.14
3.00	1.54	1.94	9.55
3.21	1.07	1.50	10.17
3.50	0.61	1.06	10.70
4.00	0.07	0.58	11.06

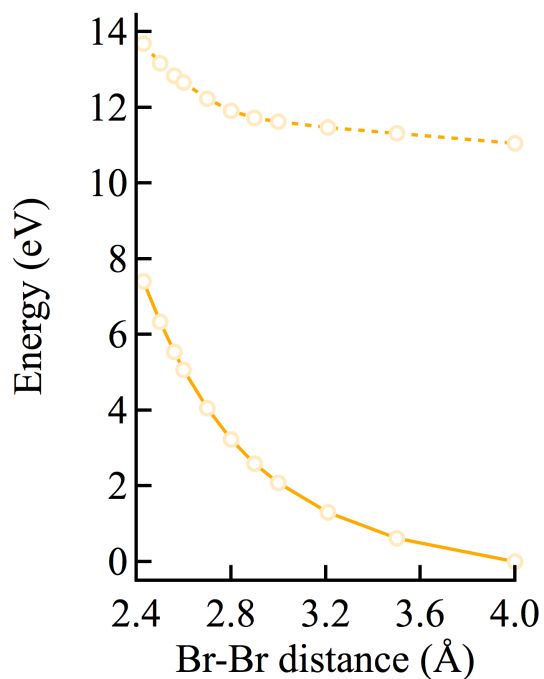


Figure S7: Ground state S_0 (black line) and first excited state S_1 (blue line) relative energies as a function of the Br-Br distance for Br_3^{3-} .